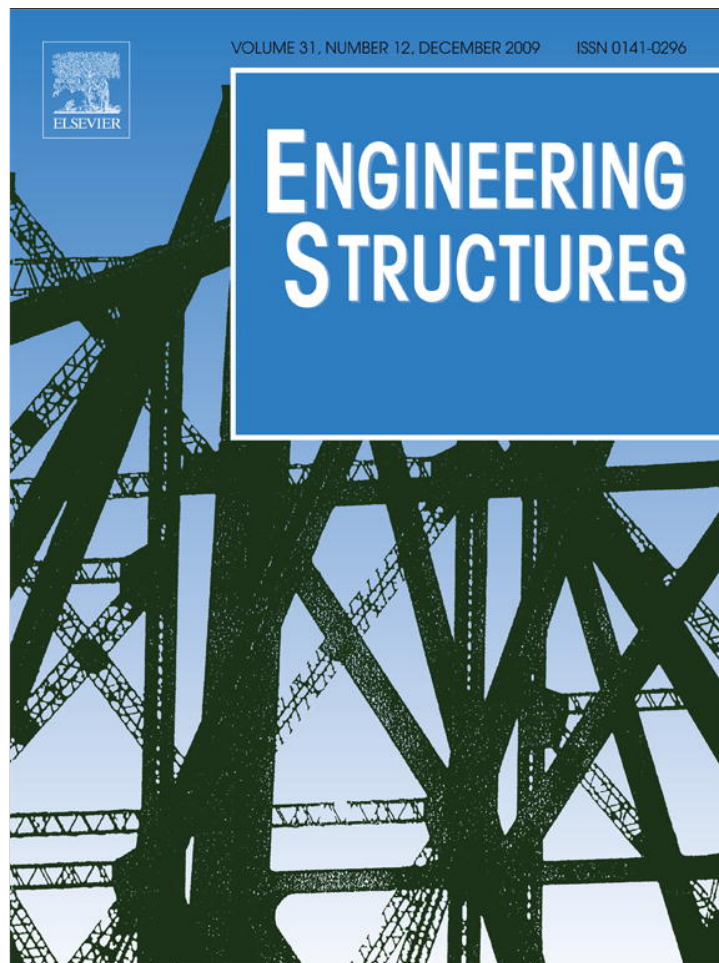


Provided for non-commercial research and education use.  
Not for reproduction, distribution or commercial use.

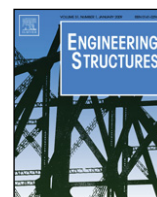


This article appeared in a journal published by Elsevier. The attached copy is furnished to the author for internal non-commercial research and education use, including for instruction at the authors institution and sharing with colleagues.

Other uses, including reproduction and distribution, or selling or licensing copies, or posting to personal, institutional or third party websites are prohibited.

In most cases authors are permitted to post their version of the article (e.g. in Word or Tex form) to their personal website or institutional repository. Authors requiring further information regarding Elsevier's archiving and manuscript policies are encouraged to visit:

<http://www.elsevier.com/copyright>



# Residual stresses in autofrettaged vessel made of functionally graded material

B. Haghpanah Jahromi<sup>a</sup>, G.H. Farrahi<sup>b</sup>, M. Maleki<sup>b</sup>, H. Nayeb-Hashemi<sup>a</sup>, A. Vaziri<sup>a,\*</sup>

<sup>a</sup> Department of Mechanical and Industrial Engineering, Northeastern University, Boston, MA, USA

<sup>b</sup> Department of Mechanical Engineering, Sharif University of Technology, Tehran, Iran

## ARTICLE INFO

### Article history:

Received 19 May 2009

Received in revised form

25 June 2009

Accepted 16 July 2009

Available online 29 July 2009

### Keywords:

Functionally graded material

Thick vessel

Autofrettage

Pressure vessels

Variable material property method

## ABSTRACT

We used an extension of the Variable Material Property method for materials with varying elastic and plastic properties to evaluate the residual stresses in an autofrettaged thick vessel made of functionally graded metal–ceramic composite. It is shown that the reinforcement of the metal vessel by ceramic particles, with an increasing ceramic volume fraction from inner to outer radius, increases the magnitude of compressive residual stresses at the inner section of an autofrettaged vessel and thus, could lead to better fatigue life and load-carrying capacity of the vessel. A parametric study is carried out to highlight the role of ceramic particle strength and spatial distribution, as well as the autofrettage pressure on the induced residual stresses in a thick vessel.

© 2009 Elsevier Ltd. All rights reserved.

## 1. Introduction

Functionally graded materials (FGMs) are novel materials which are used in a broad array of applications that range from aerospace structures and cutting tools to electronics and biomedical engineering [1–3]. FGMs, while offering the advantages of composites, avoid the negative effects of abrupt changes in the material constituent due to their unique composition. Here, we explore a new application of FGM for designing autofrettaged vessels. Autofrettage is a process in which compressive residual stresses are induced in a vessel by applying an internal pressure to the vessel that is well beyond its normal service pressure [4–6]. The induced compressive residual stress leads to enhancement of the fatigue life and load-carrying capacity of the vessel [7–10]. The performance of the autofrettaged vessel mainly depends on the magnitude of the residual compressive stress, which for metal vessels is limited by the plasticity of the metal [11]. To overcome this limitation, we propose to reinforce the metal vessel with ceramic particles with a ceramic volume fraction that varies along the vessel thickness. To analyze the residual stresses induced in a composite vessel, we extended the Variable Material Property (VMP) method developed by Jahed and Dubey [12] for materials with varying elastic and plastic properties. In the VMP method, the linear elastic solution of a boundary value problem is used as a basis to generate its inelastic solution. The material parameters are

considered as field variables and their distribution is obtained as a part of solution in an iterative manner. This method is generally employed to homogeneous elastic–plastic materials [13–15]. In this study, we have extended the application of the VMP method to materials with varying elasto–plastic properties and demonstrated its applications to calculate the residual stresses in an autofrettaged FGM vessel.

## 2. Theoretical model

We assumed that the functionally graded metal–ceramic composite is locally isotropic and yields according to the von Mises criterion. For a cylinder, the material response of an infinitesimally small element located at a distance  $x$  from its internal radius can be represented by an elastic modulus,  $E(x)$ , and Poisson ratio,  $\nu(x)$  and a curve that represents the plastic behavior of the element. The component of strain tensor,  $\varepsilon_{ij}$ , is the summation of the elastic part,  $\varepsilon_{ij}^e$ , and plastic part,  $\varepsilon_{ij}^p$ . The elastic part is given as,

$$\varepsilon_{ij}^e = \frac{1 + \nu(x)}{E(x)} \sigma_{ij} - \frac{\nu(x)}{E(x)} \sigma_{kk} \delta_{ij} \quad (1)$$

where  $\delta_{ij}$  is the Kronecker delta and the plastic part of strain is given by Hencky's total deformation equation,  $\varepsilon_{ij}^p = \phi(x, \bar{\varepsilon}^p) s_{ij}$ , where  $s_{ij} = \sigma_{ij} - \frac{1}{3} \sigma_{kk} \delta_{ij}$  is the deviatoric stress, and  $\phi$  is a scalar function given by  $\phi = \frac{3}{2} \frac{\bar{\varepsilon}^p}{\sigma_{eq}}$ , where  $\bar{\varepsilon}^p$  and  $\sigma_{eq}$  are the equivalent plastic strain and equivalent stress, respectively. Considering the above relationships, the total strain in an element can be written as,

$$\varepsilon_{ij} = \left( \frac{1 + \nu(x)}{E(x)} + \phi(x) \right) \sigma_{ij} - \left( \frac{\nu(x)}{E(x)} + \frac{1}{3} \phi(x) \right) \sigma_{kk} \delta_{ij}. \quad (2)$$

\* Corresponding author.

E-mail address: [vaziri@coe.neu.edu](mailto:vaziri@coe.neu.edu) (A. Vaziri).

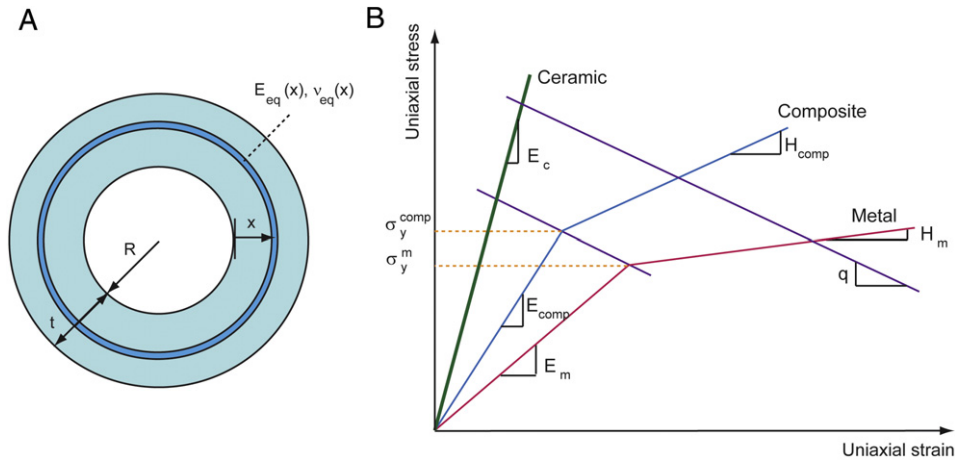


**Fig. 1.** (A) Schematic of a thick FGM vessel with internal radius  $R$  and thickness  $t$ . (B) Schematic of modified rule of mixtures used to estimate the behavior of ceramic particle-reinforced metal composite.

To analyze FGM vessels using the extended VMP method proposed here, we divided the FGM thick cylinder into thin *strips* (elements), with an equivalent elastic modulus and a Poisson ratio denoted by  $E_{eq}(x)$  and  $\nu_{eq}(x)$ , respectively, See Fig. 1(A). The components of strain tensor in each element,  $\varepsilon_{ij}^*$ , are,

$$\varepsilon_{ij}^* = \frac{1 + \nu_{eq}(x)}{E_{eq}(x)} \sigma_{ij} - \frac{\nu_{eq}(x)}{E_{eq}(x)} \sigma_{kk} \delta_{ij} \quad (3)$$

where  $x$  denotes the distance of the center line of the strip from the internal radius of the vessel. Based on the VMP method, the element has elastic strain components equal to the total strain components of the elasto-plastic element presented in Eq. (2). Comparing Eqs. (2) and (3), the following relationships are obtained:

$$\begin{aligned} E_{eq}(x) &= \frac{3E(x)}{3 + 2E(x)\phi(x)} \\ \nu_{eq}(x) &= \frac{3\nu(x) + E(x)\phi(x)}{3 + 2E(x)\phi(x)}. \end{aligned} \quad (4)$$

Eliminating  $\phi(x)$  from the above equations gives:

$$\nu_{eq}(x) = \frac{E_{eq}(x)(2\nu(x) - 1) + E(x)}{2E(x)}. \quad (5)$$

In order to evaluate the state of stress in the thick FGM vessel, first, we estimate the state of stress in each element using Lamé's equations for a pressurized hollow cylinder [16] by assuming  $E_{eq}(x) = E(x)$  and  $\nu_{eq}(x) = \nu(x)$ . Based on Lamé's equations, for each strip located at  $x$ , the inside and outside displacements,  $u_x$  and  $u_{x+dx}$ , are related to the inside and outside pressures,  $p_x$  and  $p_{x+dx}$ , by:

$$\begin{bmatrix} C_{11,x} & C_{12,x} \\ C_{21,x} & C_{22} \end{bmatrix}^{-1} \begin{Bmatrix} u_x \\ u_{x+dx} \end{Bmatrix} = \begin{Bmatrix} p_x \\ p_{x+dx} \end{Bmatrix} \quad (6)$$

where for the plane strain condition:

$$\begin{aligned} C_{11,x} &= \frac{1 + \nu_{eq}(x)}{E_{eq}(x)} \frac{(R+x)^3}{(R+x+dx)^2 - (R+x)^2} \\ &\quad \times \left( 1 - 2\nu_{eq}(x) + \frac{(R+x+dx)^2}{(R+x)^2} \right) \\ C_{12,x} &= -2 \frac{(1 - \nu_{eq}^2(x))}{E_{eq}(x)} \frac{(R+x)(R+x+dx)^2}{(R+x+dx)^2 - (R+x)^2} \end{aligned}$$

$$\begin{aligned} C_{21,x} &= -2 \frac{(1 - \nu_{eq}^2(x))}{E_{eq}(x)} \frac{(R+x)(R+x+dx)^2}{(R+x+dx)^2 - (R+x)^2} \\ C_{22,x} &= \frac{1 + \nu_{eq}(x)}{E_{eq}(x)} \frac{(R+x+dx)^3}{(R+x+dx)^2 - (R+x)^2} \\ &\quad \times \left( (1 - 2\nu_{eq}(x)) + \frac{(R+x)^2}{(R+x+dx)^2} \right). \end{aligned} \quad (7)$$

Considering that the elements' deformation satisfy the requirements of equilibrium and compatibility at their boundary in both radial and axial directions (e.g. for plane stress condition: equal interface pressure, radial compatibility, uniform axial deformation and zero total axial force), one can obtain the state of stress in the vessel from the characteristic relations between pressure and displacement for each element. Once the state of stress in the vessel is obtained,  $E_{eq}(x)$  is updated for each element based on the calculated equivalent stress by using the projection method [12]. Then, the effective Poisson ratio for each element,  $\nu_{eq}(x)$ , is obtained using Eq. (5). In the next step, the state of stress in each element is re-calculated from Eqs. (6) and (7) using the updated values of effective elastic modulus and effective Poisson ratio. This procedure is continued until the convergence to the stress solution is achieved. The numerical procedure gives an estimate of the elasto-plastic stresses in the FGM vessel due to loading.

The problem under study requires also finding the unloading solution of the FGM vessel. The unloading solution is analogous to loading with each element having its own nonlinear unloading behavior which depends on the element equivalent stress at the onset of unloading and material hardening behavior (e.g. isotropic hardening or kinematic hardening). Once the loading and unloading stresses are calculated based on the method outlined above, the residual stress field can be estimated by superposing the stress fields associated with loading and unloading solutions.

### 3. FGM mechanical behavior

The above analysis requires having the uniaxial stress-strain curves of the metal-ceramic composite with different ceramic volume fractions. Here, we assume that the metal has bilinear elastic-plastic behavior shown in Fig. 1(B), with elastic modulus,  $E_m$ , tangent modulus,  $H_m$  and yield stress under uniaxial loading,  $\sigma_y^m$ . The ceramic is assumed to have linear elastic behavior as shown schematically in Fig. 1(B) with the elastic modulus  $E_c$ . The elastic modulus of the metal-ceramic composite,  $E_{comp}$ , the overall flow strength of the composite corresponding to the onset of

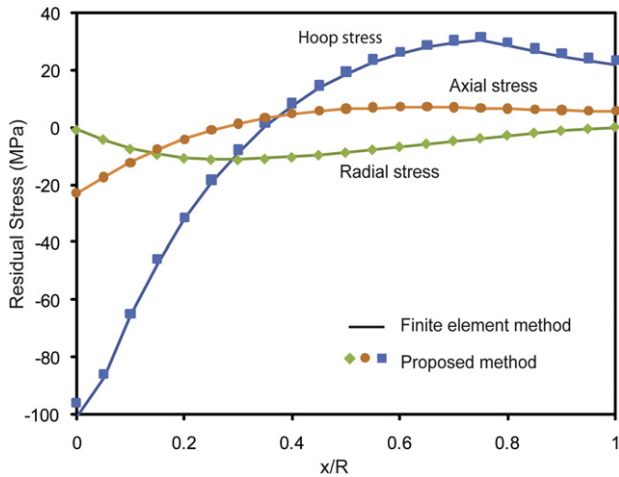


**Fig. 2.** Comparison with the finite element method. The results show the residual stresses in an autofrettagged vessel with  $f_0 = 0.8$  and  $n = 1$  subjected to autofrettagge pressure 100 MPa. In this calculation,  $E_c = 20$  GPa. The vessel has  $t/R = 1$  and plane-strain condition.

plastic yielding,  $\sigma_y^{comp}$  and the tangent modulus of the composite,  $H_{comp}$ , which represents its strain hardening behavior, can be calculated using the modified rule of mixture for composites [17] – See Fig. 1(B),

$$E_{comp} = \left[ (1-f) \left( \frac{q+E_c}{q+E_m} \right) + f \right]^{-1} \times \left[ (1-f)E_m \left( \frac{q+E_c}{q+E_m} \right) + fE_c \right]$$

$$\sigma_y^{comp} = \sigma_y^m \left[ (1-f)E_m \left( \frac{q+E_m}{q+E_c} \right) \cdot \frac{E_c}{E_m} \cdot f \right]$$

$$H_{comp} = \left[ (1-f) \left( \frac{q+E_c}{q+E_m} \right) + f \right]^{-1} \times \left[ (1-f)H_m \left( \frac{q+E_c}{q+H_m} \right) + fE_c \right] \quad (8)$$

where  $f$  denotes the volume fraction of the ceramic particles and  $q$  is the ratio of stress to strain transfer, which is a parameter that defines the metal/ceramic composite behavior [17].

In this study, the ceramic particle reinforcement is assumed to have a volume fraction that varies from 0 at the inner surface to  $f_0$  at the outer surface according to the, following relationship:

$$f(x) = f_0 \left( \frac{x}{t} \right)^n \quad (9)$$

where  $f(x)$  is the reinforcement volume fraction and  $t$  is the thickness of the vessel. In this case,  $f_0 = 0$  denotes a metal vessel and  $n = 0$  denotes uniformly-reinforced metal–ceramic vessel.

In all the calculations presented here, the metal component of the FGM has  $E_m = 56$  GPa,  $H_m = 12$  GPa,  $\sigma_y^m = 106$  MPa and the Poisson ratio is assumed to be constant and equal to 0.25 [18]. The elastic modulus of the ceramic component of FGM is varied systematically between  $\sim 5$  GPa and 560 GPa (i.e.  $0.1 < E_c/E_m < 10$ ) with constant Poisson ratio 0.25. The value of  $q$  is taken as 17.2 GPa based on the micro-indentation experiments by Gu et al. [18]. Furthermore, for calculating the loading and unloading solutions of the thick vessel during the autofrettagge process, we assumed that the metal–ceramic composite demonstrates isotropic hardening behavior.

#### 4. Results

To establish the validity of our numerical method, we compared the results of our analysis to the results obtained from finite element method. A finite element model of a vessel subjected to internal pressure was constructed using commercially available software, ANSYS. In the finite element model, the vessel was divided to twenty cylindrical layers (strips) with equal thickness. It was assumed that each layer has a constant elastic modulus, tangent modulus and yield stress, which were calculated based on the volume fraction of the ceramic at the center of the layer using Eq. (9). The model was meshed using two-dimensional, 8-node quadrilateral elements and mesh sensitivity analysis was performed to assure that the results are not sensitive to the element size. We also checked that increasing the number of layers through the thickness of the vessel does not yield any considerable change in the results. In Fig. 2, we compared a set of results from the finite element calculations obtained for the plane strain condition and the developed numerical method for a FGM vessel subjected to autofrettagge pressure 100 MPa. The results indicate that the developed numerical method is capable of calculating residual stresses in an autofrettagged vessel with high fidelity.

We used the developed model to study the residual stresses in an autofrettagged FGM vessel with various ceramic particle reinforcement distributions. All the results are presented for the plane strain condition (vessels with two fix ends). Fig. 3(A) shows the distribution of residual hoop stresses along the thickness of a uniformly-reinforced metal–ceramic vessel ( $n = 0$ ) with inner radius/outer radius = 2 and subjected to autofrettagge pressure 300 MPa. The magnitude of residual stresses significantly decreases as the volume fraction of the ceramic particles, denoted by  $f_0$ , is increased. Note that an all-ceramic vessel does not have any residual stresses, since the ceramic behavior is assumed to be elastic – see Fig. 1(A). Fig. 3(B) shows the distribution of residual hoop stresses in a FGM vessel with  $n = 0.5$  and different reinforcement distribution coefficients,  $f_0$  subjected to an autofrettagge pressure 300 MPa. The induced residual hoop stress in the FGM vessels is significantly higher than residual stresses in a metal vessel or uniformly-reinforced metal–ceramic vessel, Fig. 3(A) and (B). Even small volume fractions of ceramic reinforcement with an increasing distribution through the thickness (e.g.  $f_0 = 0.2$ ) can effectively elevate the level of compressive residual stress at the inner part of the vessel. This result can be explained considering that the outer part of a FGM vessel undergoes less plastic deformation and deforms more elastically compared to a metal vessel as the autofrettagged pressure is applied. During unloading, the outer part compresses the inner part of the vessel, resulting in an increase in the residual hoop stresses at the inner part of the vessel.

We have performed a parametric study to quantify the role of ceramic particle distribution constants (i.e.  $f_0$  and  $n$ ) on the induced residuals hoop stresses. The results are summarized in Fig. 3(C) and (D), where  $\gamma = (\text{residual hoop stress at the inner surface of FGM vessel})/(\text{residual hoop stress at the inner surface of counterpart metal vessel})$  at the same autofrettagge pressure. A FGM vessel with low reinforcement distribution exponent,  $n < 0.04$ , has  $\gamma < 1$ , with the value of  $\gamma$  decreasing by increasing the ceramic the reinforcement distribution coefficient,  $f_0$ . FGM vessels with higher reinforcement distribution exponent (i.e.  $n > 0.04$ ) have  $\gamma > 1$  with the value that monotonically increases by increasing  $f_0$ . The dependence of the residual stress on the reinforcement distribution exponent is further quantified in Fig. 3(D) for different reinforcement distribution coefficients. Increasing the reinforcement distribution coefficient from zero results in an increase in the residual compressive stress at the inner surface of the vessel till  $n \sim 0.6$  in the range studied here, with the maximum  $\gamma = 4.2$  for  $f_0 \sim 1$ . However, further increase of the

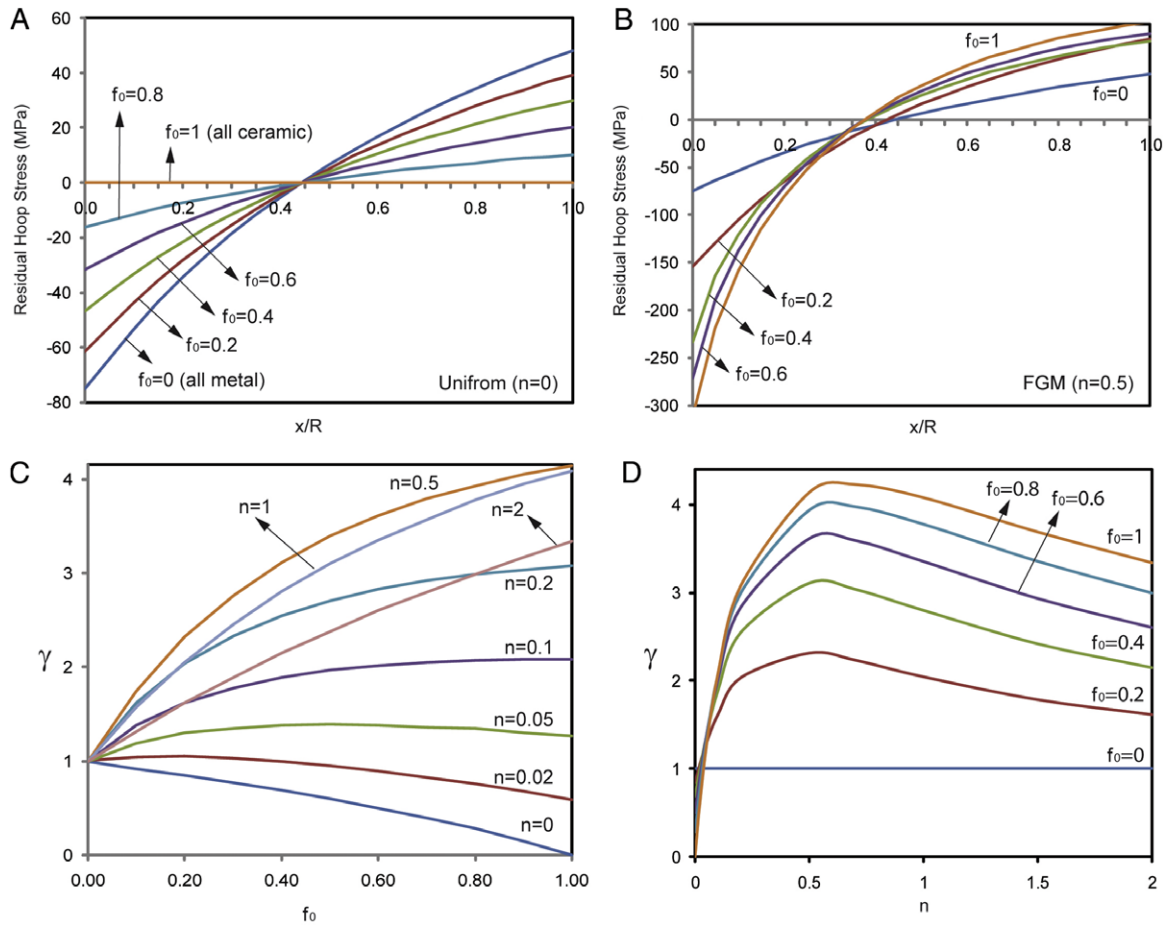


**Fig. 3.** Residual hoop stress in an autofrettaged metal–ceramic vessel. (A) Residual hoop stress of a uniformly-reinforced vessel ( $n = 0$ ) with different reinforcement distribution coefficients,  $f_0$ . (B) Residual hoop stress of a FGM vessel with  $n = 0.5$  for different  $f_0$ . (C)  $\gamma$  versus  $f_0$  for different reinforcement distribution exponents. (D)  $\gamma$  versus the reinforcement distribution exponent for different  $f_0$ . The results show that  $\gamma$  reaches its maximum value around  $n \sim 0.6$  independent of  $f_0$ . In this set of calculation,  $E_c = 80$  GPa. The vessel has  $t/R = 1$  and is subjected to autofrettage pressure 300 MPa.

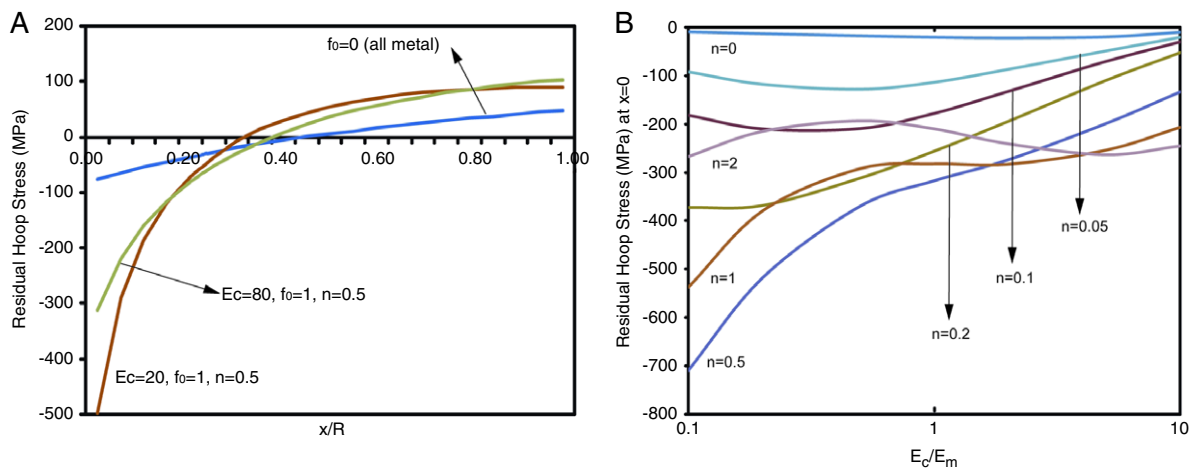


**Fig. 4.** Effect of ceramic particle stiffness. (A) Residual hoop stress along the thickness of a metal vessel and two FGM vessels reinforced with ceramic particles with two different elastic moduli. (B) Residual hoop stress at inner surface of the vessel versus the relative stiffness of the ceramic particles and metal component,  $E_c/E_m$  for  $f_0 = 0.8$  and different reinforcement distribution exponents,  $n$ . In this set of calculation, the vessel has  $t/R = 1$  and is subjected to autofrettage pressure 300 MPa.

reinforcement distribution coefficient results in a decrease in  $\gamma$ . Moreover, the induced stress is still significantly higher than the residual stress of the counterpart metal vessel.

The effect of reinforcing particle elastic modulus on the distribution of residual hoop stresses along the thickness of a FGM vessel is shown in Fig. 4(A). In this particular example, reinforcement of a FGM vessel with ceramic particles with lower elastic modu-

lus results in an increases in the value of the residual compressive stresses. To further quantify the role of ceramic particle stiffness on the residual stresses induced in the FGM vessel by the autofrettage process, we have varied the elastic modulus of the ceramic between 5.6 GPa and 560 GPa (i.e.  $0.1 < E_c/E_m < 10$ ). The results of our parametric study are displayed in Fig. 4(B) for different reinforcement distribution exponents,  $n$ . The value of  $E_c/E_m$  which

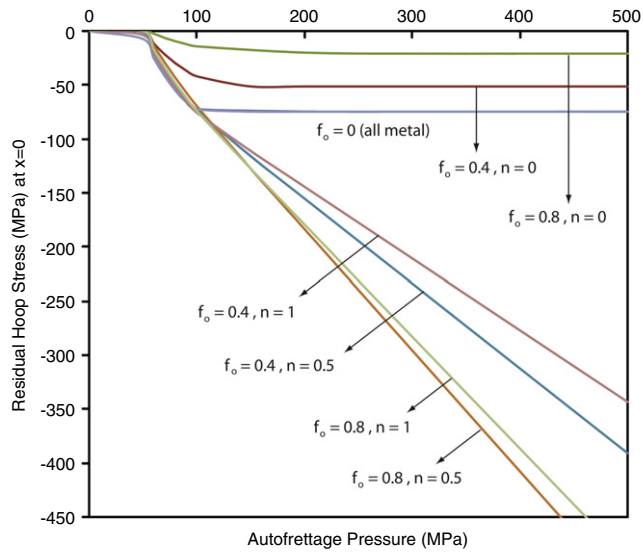


**Fig. 5.** Effect of autofrettage pressure. The results are shown for a metal vessel and a uniformly-reinforced metal–ceramic vessel ( $n = 0$ ), as well as FGM vessels with various reinforcement distribution coefficients and exponents. In this calculation,  $E_c = 80$  GPa and the vessel has  $t/R = 1$  and is subjected to autofrettage pressure 300 MPa.

results in a maximum residual stress at the inner surface of the vessel depends on  $n$ . For  $n > 1$ , the value of the induced residual is less sensitive to the ceramic elastic modulus. It is noteworthy that the maximum value of residual stress  $\sim 710$  MPa for  $n = 0.5$  and  $E_c/E_m = 0.1$  is significantly higher than the maximum residual stress in the counterpart metal vessel, which was  $\sim 75$  MPa. It should be emphasized here that the induced residual stress distribution in a FGM vessel is a complex function of metal and ceramic material properties and the autofrettage pressure. For example, reinforcement of vessels with ceramic particles with  $E_c/E_m < 1$  reduces the elastic modulus of the vessel, while increasing its yield strength. Depending on the magnitude of autofrettage pressure and the reinforcement distribution exponent, the induced residual stresses could be either higher or lower than a metal vessel counterpart. We also studied the role of autofrettage pressure on the induced residual stresses in a FGM vessel. Selected set of results are shown in Fig. 5 for a wide range of autofrettage pressure and compared with the value of residual stresses in a metal vessel ( $f_0 = 0$ ) and uniformly-reinforced metal–ceramic vessels ( $n = 0$ ). The results clearly highlight another advantage of autofrettaged FGM vessels: The maximum possible value of the residual stress for metal and uniformly-reinforced composite vessels is limited by the metal plasticity and is independent of the autofrettage pressure (e.g. for a metal vessel in this case, the maximum possible value of the residual stress  $\sim 75$  MPa, which is achieved at the autofrettage pressure  $\sim 100$  MPa – further increase in the autofrettage pressure does not increase the compressive stress). However, FGM vessels do not exhibit such a limitation and the residual compressive stress at the inner part of the vessel increases by increasing the autofrettage pressure. Finally, we investigated the effect of vessel thickness on the residual hoop stresses induced in the autofrettage process. Fig. 6 shows the residual hoop stress at the vessel inner surface versus the vessel thickness normalized by its inner radius,  $t/R$ , for three different vessels:  $f_0 = 0$  (all metal),  $f_0 = 0.4$ ,  $n = 0$  (uniformly-reinforced metal–ceramic vessel), and  $f_0 = 0.8$ ,  $n = 1$  (FGM). For all metal or uniformly-reinforced metal–ceramic vessels, the maximum value of the compressive residual stress plotted in Fig. 6 is achieved at to a critical thickness/radius, where the vessel undergoes plastic deformation over its entire thickness at

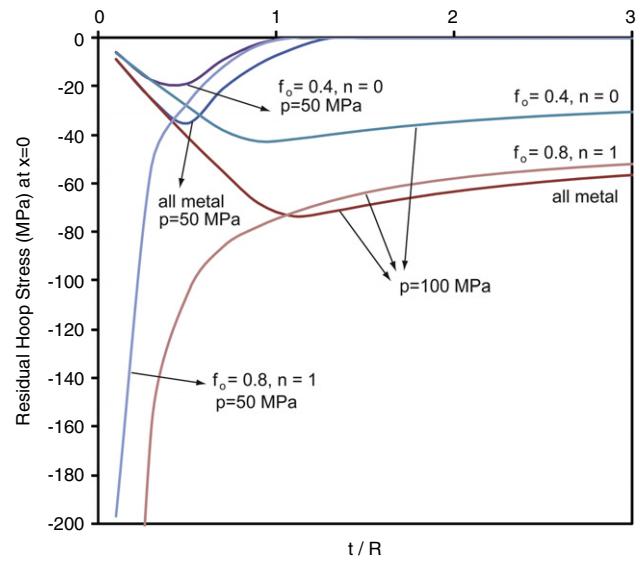


**Fig. 6.** Effect of vessel thickness. Residual hoop stress at the inner surface of the vessel versus the normalized thickness of the vessel,  $t/R$ , for three different ceramic distributions:  $f_0 = 0$  (all metal);  $f_0 = 0.4$ ,  $n = 0$  (uniformly-reinforced metal–ceramic vessel);  $f_0 = 0.8$ ,  $n = 1$  (FGM). The results are plotted for two autofrettage pressures 50 MPa and 100 MPa and  $E_c = 80$  GPa.

a given autofrettage pressure. For  $t/R$  smaller than this pressure-dependent critical thickness/radius ratio, the residual stress does not increase by increasing the autofrettage pressure since the vessel undergoes complete plastic deformation through its thickness. It is also notable that for small values of autofrettage pressure (e.g. 50 MPa in Fig. 6), the residual stress at the inner surface of the vessel decreases by increasing  $t/R$  and reaches zero since no yielding occurs in the vessel. However, at higher values of pressure, an inner part of the vessel always deforms plastically during the loading phase of the autofrettage process, inducing residual stresses during the unloading phase regardless of the vessel thickness. Moreover, for all metal and uniformly-reinforced metal–ceramic vessels the residual hoop stress approaches zero for small values of  $t/R$  due to the quasi-uniform distribution of the stresses through the vessel thickness during the loading and unloading phases. However, for a functionally graded vessel, the residual hoop stress increases as  $t/R$  decreases.

## 5. Conclusion

We investigated the residual compressive stresses induced in an autofrettaged vessel made of functionally graded metal–ceramic composite by developing an extension of the Variable Material Property method for materials with varying elastic and plastic properties. Our analysis complements the previous results on elastic and elasto-plastic analysis of FGM vessels [19–21], while allowing systematic analysis of the residual stresses in autofrettage vessels. The results of our work suggest that the reinforcement of metal vessels with ceramic particles with an increasing volume fraction through its radius – even in small quantities – increases the compressive stresses induced by the autofrettage process. Since the fatigue life and load-carrying capacity of autofrettaged vessels depend on the induced residual stresses, functionally graded materials can provide new opportunities for enhancing the performance of autofrettaged vessels. Another potential advantage of metal–ceramic FGM vessels is that the high ceramic content at the outer surface of the vessel provides enhanced thermal and corrosion protection as discussed in [22,23]. It should be noted that the parametric study presented here does not offer a general conclusion for selecting the optimum material configuration of reinforced

autofrettaged vessels. However, enough insight for selecting the near-optimized reinforced configurations is provided.

### Acknowledgment

This work was supported in part by the Department of Mechanical and Industrial Engineering, Northeastern University.

### References

- [1] Miyamoto Y, Kaysser WA, Rabin BH, Kawasaki A, Ford RG. Functionally graded materials: Design, processing, and applications. Boston (MA): Kluwer Academic Publishers; 1999.
- [2] Pompe W, Worch H, Epple M, Friess W, Gelinsky M, et al. Functionally graded materials for biomedical applications. *Mater Sci Eng A* 2003;362:40–60.
- [3] Nui X, Rahbar N, Farias S, Soboyejo WO. Bio-inspired design of dental multilayers: Experiments and model. *J Mech Behav Biomed Mater* [in press].
- [4] Farrahi GH, Hosseinian E, Assempour A. General variable material property formulation for the solution of autofrettaged thick-walled tubes with constant axial strains. *ASME Int J Press Vessel Technol* 2008;130.
- [5] Manning WRD, Labrow S. High pressure engineering. London: CRC Press; 1971.
- [6] Chen PCT. Stress and deformation analysis of autofrettaged high pressure vessels. In: ASME special publication, vol. 110. ASME United Engineering Center; 1986. p. 61–7.
- [7] Parker AP, Underwood JH. Influence of the bauschinger effect on residual stress and fatigue lifetimes in autofrettaged thick-walled cylinders. *Fat Fract Mech* 1997;29.
- [8] Webster GA, Ezeilo AN. Residual stress distributions and their influence on fatigue lifetimes. *Int J Fat* 2001;23:S375–83.
- [9] Rees DWA. The fatigue life of thick-walled autofrettaged cylinders with closed ends. *Fract Eng Mater Struct* 1991;14:51–68.
- [10] Suresh S. Fatigue of materials. second ed. UK: Cambridge University Press; 1998.
- [11] Koh SK. Fatigue crack growth life of thick-walled cylinders with an external radial crack. *Fat Fract Eng Mater Struct* 1996;19:15–25.
- [12] Jahed H, Dubey RN. An axisymmetric method of elastic-plastic analysis capable of predicting residual stress field. *J Pressure Vessel Technol* 1997;119:264–73.
- [13] Jahed H, Farshi B, Karimi M. Optimum autofrettage and shrink-fit combination in multi-layer cylinders. *J Press Vessel Technol* 2006;128:196–201.
- [14] Jahed H, Farshi B, Bidabadi J. Minimum weight design of inhomogeneous rotating discs. *Int J Press Vessels Pip* 2005;82:35–41.
- [15] Jahed H, Shirazi R. Loading and unloading behaviour of a thermoplastic disc. *Int J Press Vessels Pip* 2001;78:637–45.
- [16] Timoshenko SP, Goodier JN. Theory of elasticity. third ed. McGraw-Hill; 1970.
- [17] Suresh S, Mortensen A. Fundamentals of functionally graded materials. London: IOM Communications Ltd; 1998.
- [18] Gu Y, Nakamura T, Prchlik L, Sampath S, Wallace J. Micro-indentation and inverse analysis to characterize elastic-plastic graded materials. *Mater Sci Eng A* 2003;345:223–33.
- [19] Tutuncu N. Stresses in thick-walled FGM cylinders with exponentially-varying properties. *Eng Struct* 2007;29:2032–5.
- [20] Figueiredo F, Borges L, Rochinha F. Elasto-plastic stress analysis of thick-walled FGM pipes. *AIP Conf Proc* 2008;973:147–52.
- [21] Eraslan AN, Akis T. Plane strain analytical solution of functionally graded elastic-plastic pressurized tube. *Int J Press Vessels Pip* 2006;83:635–44.
- [22] Schulz U, Peters M, Bach F-W, Tegeder G. Graded coatings for thermal, wear and corrosion barriers. *Mater Sci Eng A* 2003;362:61–80.
- [23] Suresh S. Graded materials for resistance to contact deformation and damage. *Science* 2001;292:2247–51.